Phase Dependence of Enhanced Ionization in Asymmetric Molecules

G. Lagmago Kamta and A. D. Bandrauk

Département de Chimie, Université de Sherbrooke, Sherbrooke, Québec, Canada, J1K 2R1

(Received 6 February 2005; published 27 May 2005)

We study enhanced ionization (EI) in asymmetric molecules by solving the 3D time-dependent Schrödinger equation for HeH^{2+} driven by a few-cycle laser pulse linearly polarized along the molecular axis. We find that EI is much stronger when the laser's carrier-envelope phase is such that the electric field at the peak of the pulse is antiparallel to the permanent dipole of the molecule (PDM). This phase dependence is explained by studying the molecule in the presence of a static electric field. When this field is antiparallel to the PDM, the energy of the dressed ground state moves up (with increasing internuclear distance R) to cross with excited states, leading to a stronger ionization via intermediate state resonances and via tunneling. We predict analytically the laser and molecular parameters at which these crossings are expected to occur in any asymmetric molecule.

DOI: 10.1103/PhysRevLett.94.203003 PACS numbers: 33.80.Eh, 33.80.Rv, 33.80.Wz, 42.50.Hz

When molecules interact with intense laser fields linearly polarized along the molecular axis, there is a critical internuclear separation at which a strong increase in the ionization rate occurs. This effect, known as enhanced ionization (EI), has been predicted [1–4] and indirectly [5] and directly [6,7] observed in experiments. With current technology, one can generate ultrashort laser pulses with fewer than two optical cycles at the full-width at half maximum (FWHM) of the pulse envelope [8]. The peak electric field of such few-cycle pulses (FCPs) depends on the carrier-envelope phase (CEP) [8]. Thus, a sensitivity to the CEP is expected for field-dependent processes such as photoionization [9,10] and harmonic generation [11]. However, for atoms and symmetric molecules interacting with linearly polarized pulses, the total ionization is invariant when the CEP is changed by 180° (or equivalently when the system is rotated by 180°), due to the inversion symmetry in such systems.

As the simplest heteronuclear asymmetric molecule, HeH^{2+} has been the subject of many experimental and theoretical works (see, e.g., [12,13], and references therein). Because of the strong nuclei repulsion, the ground state ($1s\sigma$) and most electronic states of HeH^{2+} are repulsive. The lowest electronic bound state of HeH^{2+} is the first excited state $2p\sigma$, whose potential curve has a minimum 0.849 eV deep at the internuclear distance of $3.89a_0$ [13].

In this Letter, we perform a fixed nuclei three-dimensional study of the ionization of HeH^{2+} by a FCP (4 fs, 400 nm) linearly polarized along the internuclear axis z. We consider two CEPs leading to two configurations in which the electric field at the peak of the FCP is parallel and antiparallel to the PDM. We find that EI occurs in both configurations, but it is much stronger for the latter. This new effect is explained by studying the molecule in a static field oriented parallel (the P orientation) and antiparallel (the A orientation) to PDM. We find that with increasing R, the ground state energy of the system in the static field goes downhill for the P orientation; whereas for the A orientation the ground state energy moves up to cross with excited states, thereby enhancing various ionization mechanisms (field and tunnel ionization, and ionization via resonances with excited states). We also use the field ionization model of Codling *et al.* [1] for double well potentials to provide another explanation for the effect.

The time-dependent Schrödinger equation (TDSE) for HeH^{2+} in a laser field is $i\frac{\partial}{\partial t}\Psi(\mathbf{r},t)=[H+\mathbf{A}(t)\cdot\mathbf{p}]\Psi(\mathbf{r},t)$, where $H=\mathbf{p}^2/2+V(r)$ is the electronic Hamiltonian, $V(r)=-Z_1/|\mathbf{r}+\mathbf{R}/2|-Z_2/|\mathbf{r}-\mathbf{R}/2|$ is the Coulomb potential felt by the electron, and $Z_1=2e$ and $Z_2=e$ are the electric charges of He^{2+} and H^+. Atomic units (a.u.) are used. $\mathbf{R}$ is the internuclear vector. $\mathbf{A}(t,\phi)=A_0 f(t)\times\sin(\omega t+\phi)\mathbf{e}_z$ is the vector potential of the laser. A_0 is the maximum amplitude, $f(t)$ is the pulse envelope, ω is the laser frequency, ϕ is the CEP, and $\mathbf{e}_z$ is the unit vector along the z axis.

To solve the TDSE, we use the spheroidal coordinate system and expand $\Psi(\mathbf{r},t)$ in a complex basis as: $\Psi(\xi,\eta,t)=\Sigma_{\mu,\nu}a_{\mu\nu}(t)U_\nu(\xi)V_\mu(\eta)$, where $a_{\mu\nu}(t)$ are time-dependent coefficients, $U_\nu(\xi)=\sqrt{2\beta R}e^{-\beta R(\xi-1)}\times L_\nu[2\beta R(\xi-1)]$ and $V_\mu(\eta)=\sqrt{(\mu+1/2)}P_\mu(\eta)$. $\mu=0,1,2,\ldots,\mu_{\max}$; and $\nu=0,1,2,\ldots,\nu_{\max}$. $L_p(x)$ and $P_p(x)$ are Laguerre and Legendre polynomials, respectively. See [14–16] for more details on the complex basis expansion used.

In the above basis expansion, the TDSE becomes the system of equations $i\frac{\partial}{\partial t}\mathbf{S}\Psi=[\mathbf{H}+A(t)\mathbf{D}]\Psi$, where $\mathbf{S}$, $\mathbf{H}$, and $\mathbf{D}$, respectively, denote the overlap, the atomic Hamiltonian, and the momentum operator matrices. Ψ is the vector representation of the wave function. We solve the system using a semi-implicit Rosenbrock method [17]. We also solve the eigenvalue problem $\mathbf{H}\Phi=E\mathbf{S}\Phi$, which yields discrete electronic energies E_n, and the corresponding wave functions Φ_n. Negative energy states ($E_n<0$) correspond to bound electronic states and positive energy states ($E_n>0$) correspond to discretized continuum elec-

tronic states. The total ionization probability $P_{\rm ion}$ is extracted from the wave function $\Psi(t_{\rm end})$ at the end of the laser pulse as $P_{\rm ion} = 1 - \sum_{n(E_n<0)} |\langle \Phi_n | \Psi(t_{\rm end}) \rangle|^2$, where the summation runs over all bound states.

Our results are obtained using the basis parameters $|\beta| = 0.2$, $\theta = 0.1$, $\mu_{\rm max} = 35$, and $\nu_{\rm max} = 80$, which correspond to 2916 basis functions. The initial state for time propagation is the $1s\sigma$ state of HeH^{2+}. We use a cosine squared envelope $f(t)$, and a laser frequency $\omega = 0.114$ a.u. ($\lambda = 400$ nm). The pulse duration is 1.5 periods at the FWHM of the pulse, i.e., a total of 3 periods (4 fs).

Figure 1 shows the electric field $E(t, \phi) = -\frac{\partial}{\partial t} A(t, \phi)$ of the laser for the CEPs $\phi = 0$ and $\phi = \pi$, and the ionization probability for peak intensities 5×10^{15} and 10^{15} W/cm^2. One sees that EI occurs in all cases, as the ionization probability increases sharply when some critical

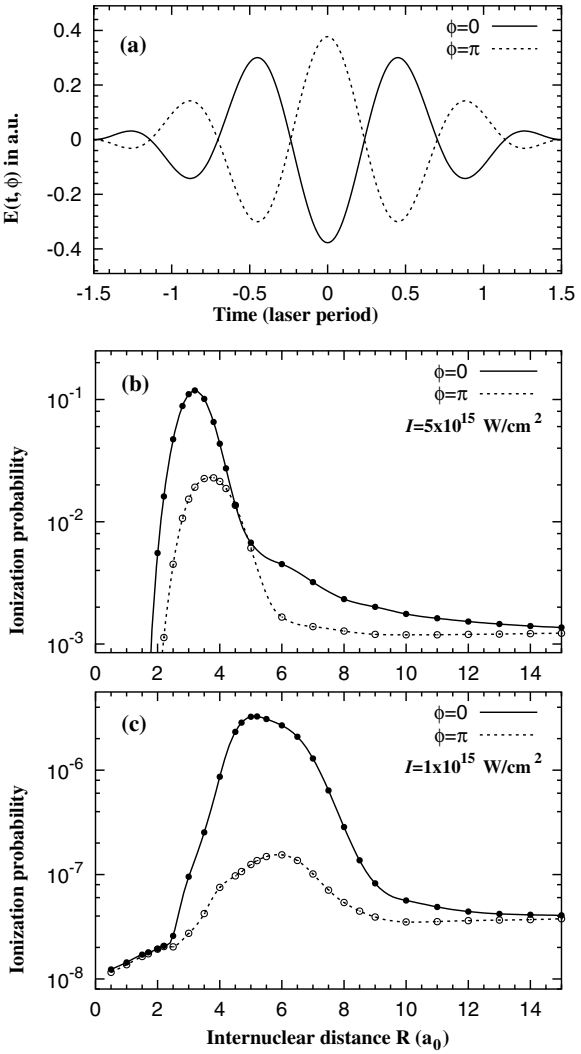

FIG. 1. (a) $E(t, \phi)$ for CEPs $\phi = 0$ and $\phi = \pi$, and peak intensity 5×10^{15} W/cm^2. Ionization probability of HeH^{2+} for the two CEPs and two peak intensities: (b) 5×10^{15} W/cm^2; (c) 10^{15} W/cm^2. Circles are the calculated data, the lines are drawn to guide the eye.

internuclear distance is reached (about $3a_0$ for 5×10^{15} W/cm^2 and $5a_0$ for 10^{15} W/cm^2). Moreover, in a stark contrast to the case of symmetric molecules, EI is stronger for $\phi = 0$ than for $\phi = \pi$, independently of the laser's peak intensity. This asymmetry in EI progressively disappears with increasing pulse duration [18].

A characteristic feature of FCPs in Fig. 1(a) is that the electric field at the peak of the pulse dominates that of all other subpeaks. Thus, as far as ionization is concerned, a strong component of the system's response to the FCP is similar to a response to a static field F oriented in the same direction as the electric field at the peak of the pulse. Such a field corresponding to $\phi = 0$ is antiparallel to the PDM [see Fig. 2(a)]; whereas the static field corresponding to $\phi = \pi$ is parallel to the PDM [see Fig. 2(b)]. To explain the asymmetry in EI, we diagonalize (in the complex basis) the Hamiltonian $H + Fz$ for the system in the field F. The resulting eigenvalues (the quasienergies) are complex: their real parts are the energies of the system dressed by the field [14].

Figure 3 shows the energies of the $1s\sigma^*$ and $2p\sigma^*$ states dressed by the static field vs R, for the P and A orientations and for various field strengths: $|F| = 0.38$ a.u. (5×10^{15} W/cm^2), $|F| = 0.29$ a.u. (3×10^{15} W/cm^2), $|F| = 0.17$ a.u. (10^{15} W/cm^2), and $|F| = 0.12$ a.u. (5×10^{14} W/cm^2). One sees that for the A orientation [Figs. 3(a), 3(c), 3(e), and 3(g)] the energy of the dressed ground state $1s\sigma^*$ moves upward with increasing R and intersects with that of the lowest excited state $2p\sigma^*$, which is moving downward. On its way up, the energy of $1s\sigma^*$ also crosses many other dressed excited states (not shown) located above $2p\sigma^*$. In contrast, for the P orientation, the $1s\sigma^*$ state energy moves downward with increasing R, and avoids crossing with any excited state.

With increasing R, the $1s\sigma$ state energy in the absence of external field is increasingly closer to $-I_1 = -Z_1^2/2$, whereas the energy of the $2p\sigma$ tends to $-I_2 = -Z_2^2/2$, where I_1 and I_2 are the ionization potentials of He^+ and H. With Fig. 4 in mind, this means that the $1s\sigma$ and $2p\sigma$ states

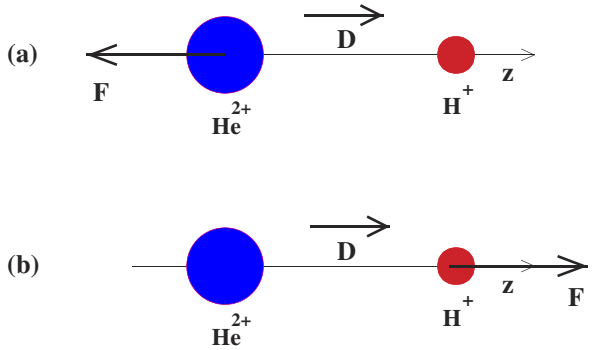

FIG. 2 (color online). The two possible configurations in which HeH^{2+} can be aligned relative to a static electric field **F**. The direction of the permanent dipole **D** of the molecule is also shown. (a) The A orientation, (b) the P orientation.

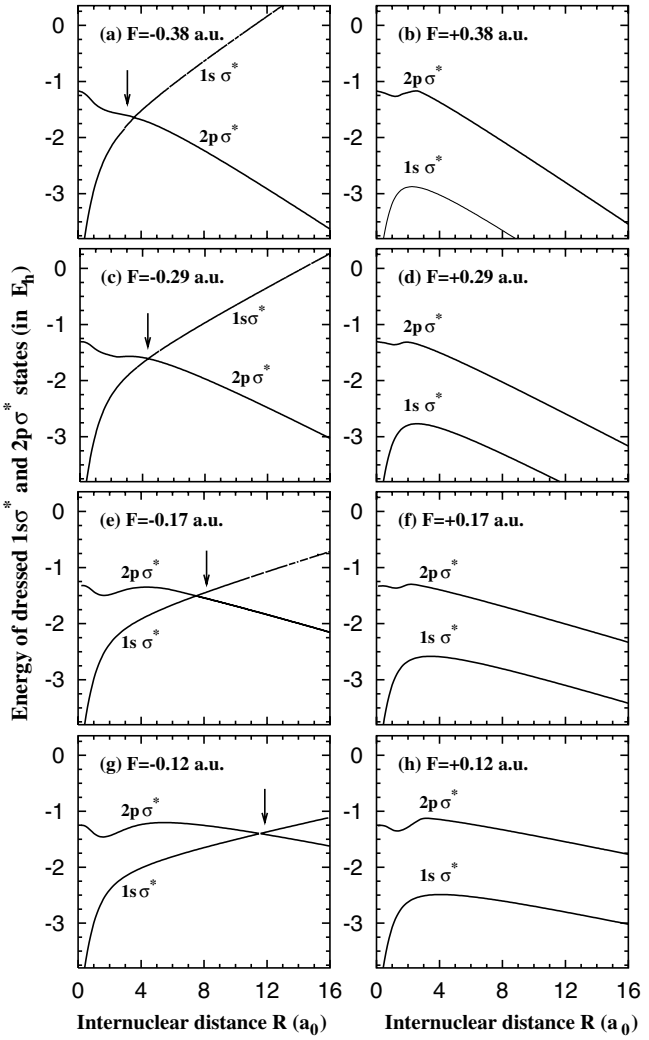

FIG. 3. Energies of the dressed states $1s\sigma^*$ and $2p\sigma^*$ of HeH^{2+} in a static field $\mathbf{F}$ of various magnitudes and orientations shown. Left plots (a),(c),(e),(g) are for the A orientation (i.e., $F < 0$) shown in Fig. 2(a); and right plots (b),(d),(f),(h) are for the P orientation (i.e., $F > 0$) shown in Fig. 2(b). The superscript $*$ indicates that the state is dressed by the field. Vertical arrows indicate the location of the crossings as predicted by Eq. (1).

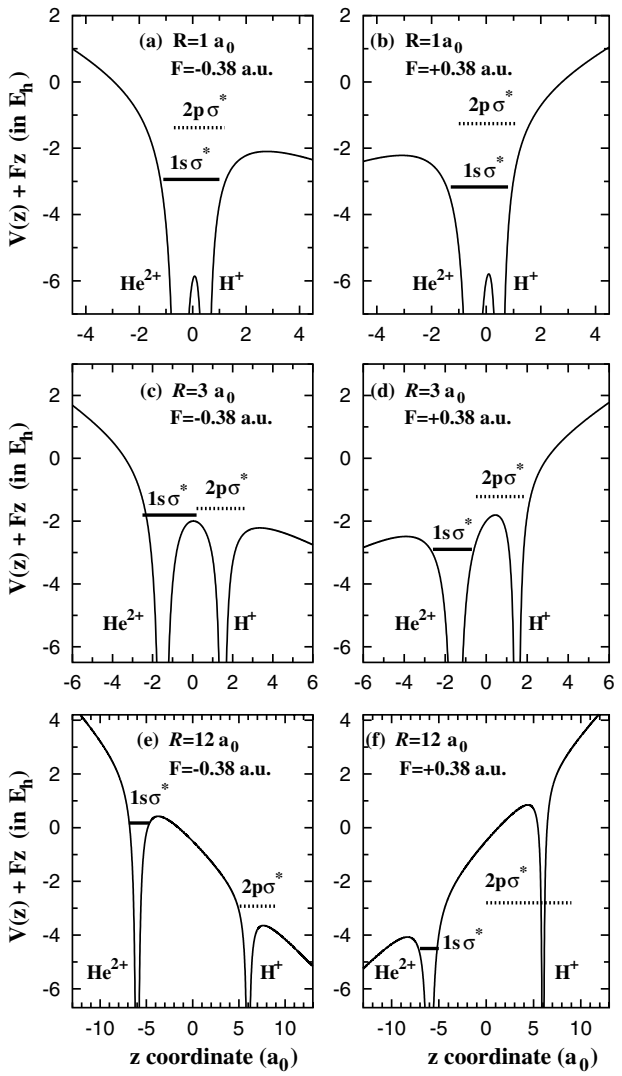

FIG. 4. Combined Coulomb and static field potentials $V(r) + E(t, \phi)z$ for HeH^{2+} along the z axis for various Rs ($R = 1a_0$, $R = 3a_0$, and $R = 12a_0$) and orientations of a static field $\mathbf{F}$ of strength $|\mathbf{F}| = 0.38$ a.u. ($I = 5 \times 10^{15}$ W/cm^2). Left plots correspond to the A orientation ($F < 0$), and right plots to the P orientation ($F > 0$). Energy levels of the field-dressed $1s\sigma^*$ (solid lines) and $2p\sigma^*$ (dashed lines) states are shown.

become increasingly located on the left and right potential wells, respectively. For R large enough for the inner potential barrier to be non-negligible, the energy of the electron in the left potential well in the A orientation [see, e.g., Fig. 4(c)] can be approximated by $E_L = -I_1 - Z_2/R + |F|R/2$: i.e., the electron energy in the field of He^{2+} ($-I_1$), lowered by the Coulomb potential of the neighboring H^+ ion ($-Z_2/R$), and increased by the uplifting action of the field strength ($|F|R/2$). Similarly, one may approximate the energy of the electron in the right potential well by $E_R = -I_2 - Z_1/R - |F|R/2$. The energy crossing occurs when $E_L = E_R$, which gives two solutions: one solution leads to internuclear distances smaller than $1a_0$, which is within the united atomic limit where the inner potential barrier is almost nonexistent. Thus, we only retain the other solution

$$R_{\mathrm{cr}} = \frac{(I_1 - I_2) + \sqrt{(I_1 - I_2) - 4|F|(Z_1 - Z_2)}}{(2|F|)}, \qquad (1)$$

as the internuclear distance at which crossings are expected to occur. Equation (1) predicts the location of crossings remarkably well (see vertical arrows in Fig. 3), compared to quantum mechanical results in Fig. 3.

Results in Fig. 3 explain the stronger EI for $\phi = 0$. Indeed, the fact that with increasing R the dressed ground state moves up to cross with excited states enhances the ionization mechanism via intermediate resonances with

excited states. In this case, more population is pumped in excited states, from which ionization is stronger via multiphoton or tunneling processes. This ionization mechanism is weaker for $\phi = \pi$ (P orientation), due to the ground state moving down and avoiding excited states. This is confirmed by a much stronger excitation probability obtained for $\phi = 0$ than for $\phi = \pi$ [18].

We now discuss the stronger EI for $\phi = 0$ vs $\phi = \pi$ in the context of tunnel ionization, following the molecular double well model [1–4]. At small R [see Figs. 4(a) and 4(b)], the ground state energy is well above the maximum of the inner barrier. Thus, ionization is similar for A and P orientations, and also similar to that of an atomic ion. As the ions move apart, the field acts over a larger distance and is more effective in lowering/raising the potential barriers. For large R [see, e.g., Figs. 4(e) and 4(f)], electrons are increasingly localized on one or the other ion, due to the raising and widening inner barrier between the two wells. This hinders tunneling between the two wells, and the ionization becomes atomiclike.

At some intermediate R [see Figs. 4(c) and 4(d)] the ionization is enhanced in both A and P orientations because the electron can tunnel across or fly above the narrow inner potential barrier into the continuum. Even if tunneling from the ground state is less likely, the strong coupling between the ground state and low-lying excited states populates the latter, from which the electron can easily tunnel or fly above the potential barriers into the continuum [2], also boosting ionization. However, asymmetric molecules have the distinctive feature that the electron cloud is predominantly localized on the most electronegative ion. For the A orientation [see, e.g., Fig. 4(c)], the electron cloud of the ground state, predominantly localized on the left well, is lifted up by the field and tunnels through or flies above the thin internuclear potential barrier to reach the continuum. In contrast, for the P orientation [see, e.g., Fig. 4(d)], the electron cloud in the ground state is still localized on the left potential well, but its energy level is dragged down by the field, so that the electron tunnels instead through a wider left potential barrier to ionize. This also explains the stronger enhanced ionization for $\phi = 0$ than for $\phi = \pi$.

Specifically, Figs. 4(c) and 4(d) show the potentials for $F = 0.38$ a.u., and for $R = 3a_0$, at which EI is maximum for $\phi = 0$ [Fig. 1(b)]. One sees that both $1s\sigma^*$ and $2p\sigma^*$ energy levels are above the inner and the right potential wells [Fig. 4(c)], leading obviously to a stronger ionization than for the P orientation [Fig. 4(d)] where only the $2p\sigma^*$ level is above the inner and left potential wells.

In summary, EI in asymmetric diatomic molecules depends strongly on the CEP of FCPs. Here, we have considered two CEPs corresponding to the parallel and antiparallel orientations of the permanent dipole of the molecule relative to the peak electric field of the FCP. We have found that EI is much stronger for the antiparallel orientation than for the parallel orientation. Simulations performed for a static electric field provide an explanation for this new effect: Because the electron cloud in asymmetric diatomic molecules tends to be displaced on one nucleus, the energy level of the dressed ground state is moved downward by the electric field for the parallel orientation. Instead, for the antiparallel orientation, the ground state energy level is lifted up to cross with excited states, leading to a larger ionization via tunneling and via intermediate resonances with excited states. Since this phase dependence of EI results essentially from the existence of an asymmetric potential well, we expect this effect to occur in any nonsymmetric polar molecule.

We thank the Natural Sciences and Engineering Research Council of Canada (NSERC) and the Canadian Institute for Photonics Innovation (CIPI) for their financial support.

[1] K. Codling *et al.*, J. Phys. B **22**, L331 (1989); K. Codling and L. J. Frasinski, J. Phys. B **26**, 783 (1993).
[2] T. Zuo and A. D. Bandrauk, Phys. Rev. A **52**, R2511 (1995); T. Zuo *et al.*, Phys. Rev. A **48**, 3837 (1993).
[3] T. Seideman *et al.*, Phys. Rev. Lett. **75**, 2819 (1995).
[4] S. Chelkowski and A. D. Bandrauk, J. Phys. B **28**, L723 (1995).
[5] M. Schmidt *et al.*, Phys. Rev. A **50**, 5037 (1994); D. Normand and M. Schmidt, Phys. Rev. A **53**, R1958 (1996).
[6] E. Constant *et al.*, Phys. Rev. Lett. **76**, 4140 (1996).
[7] G. N. Gibson *et al.*, Phys. Rev. Lett. **79**, 2022 (1997).
[8] T. Brabec and F. Krausz, Rev. Mod. Phys. **72**, 545 (2000).
[9] S. Chelkowski *et al.*, Phys. Rev. A **70**, 013815 (2004).
[10] G. G. Paulus *et al.*, Nature (London) **414**, 182 (2001).
[11] A. de Bohan *et al.*, Phys. Rev. Lett. **81**, 1837 (1998); R. M. Potvliege *et al.*, J. Phys. B **33**, L743 (2000).
[12] T. Kirchner, Phys. Rev. Lett. **89**, 093203 (2002).
[13] I. Ben-Itzhak *et al.*, Phys. Rev. A **54**, 474 (1996); **49**, 1774 (1994); Phys. Rev. Lett. **71**, 1347 (1993).
[14] Z. Mulyukov *et al.*, Phys. Rev. A **54**, 4299 (1996).
[15] G. Lagmago Kamta and A. D. Bandrauk, Phys. Rev. A **70**, 011404(R) (2004); Phys. Rev. A **71**, 053407 (2005).
[16] G. Lagmago Kamta and A. D. Bandrauk, Laser Phys. **15**, 502 (2005).
[17] W. H. Press *et al.*, *Numerical Recipes in Fortran: The Art of Scientific Computing* (Cambridge University Press, Cambridge, England, 1992), 2nd ed.
[18] G. Lagmago Kamta and A. D. Bandrauk (to be published).